
Influence of thickness and temperature on the properties of Cu₂S thin films

M. Ramya^{1*} and S. Ganesan²

¹*Department of Physics, Sri Shakthi Institute of Eng. & Tech., Coimbatore 641 062, Tamil Nadu, India*

²*Department of Physics, Government College of Technology, Coimbatore 641 013, Tamil Nadu, India*

E-mail: ramsthangam@gmail.com

Abstract

Copper Sulphide (Cu₂S) thin films at different thicknesses and annealing temperatures were deposited onto glass substrate by vacuum evaporation method. XRD study reveals the phase transformation of Cu₂S film at higher thickness. Optical and resistivity study show the phase transformation of the film from Cu₂S to CuS when they are annealed at higher temperature. SEM study exhibits the disappearance of large size particles of annealed film. Stability of the film is controlled when the films are prepared at higher thickness. Optical band gap and activation energy for different thickness and various annealing temperatures of Cu₂S thin film were calculated and the values are reported. Photocurrent enhances with film thickness and heat treatment.

Keywords: Vacuum evaporation; annealing temperature; phase transformation; optical properties; resistivity properties and photocurrent

1. Introduction

As an important semiconductor with unique electronic, optical and chemical properties copper sulphide is a promising material with potential applications in many fields [1]. Copper Sulphide is a representative of II-VI chalcogenide semiconductor with unique characteristics of photo electricity transformation. Cu_{2-x}S is a p-type semiconductor in which the copper vacancies act as acceptors [2], indicating the strong dependence of electrical properties upon the density amount of copper atom in Cu_{2-x}S. It has distinct composition because of the variation in X, 1<x<2, with different stoichiometry such as Cu₂S (chalcocite), Cu_{1.96}S(djurlite), Cu_{1.8}S(digenite), Cu_{1.75}S (anilite) and CuS (Co-Vellite) where their structural and optical properties strongly depend on Cu-Defect density [3, 4]. Copper Sulphide is found to exist in two forms at room temperature as 'Copper-rich' and 'Copper-poor' phase where copper rich phases exist as chalcocite, djurlite, digenite and anilite and copper poor phase exists as co-vellite. Cu₂S has three phases; (orthorhombic, below 100^o C), (hexagonal, between 100^o C and 425^oC) and (cubic, above 425^oC). Cu_{2-x}S is a fast super ionic conductor with structural disorder, and is a potential material in the field of thermoelectric and photoelectric transformers and high temperature

thermistors [5]. Copper Sulphide provides an opportunity to fabricate p-n hetero junction for transparent semiconductor devices. Cu₂S has direct band gap energy and indirect band gap energy at 1.2eV and 1.8eV respectively, and is favorable for light absorption under sunlight illumination. Among the copper sulphides some can be used as P-type semiconductor component of solar cells, cold cathodes, sensor and nano-scale switches because of copper vacancies within lattice [6, 7]. Besides its extensive potential applications as electro conductive coatings [8], solar control coatings [9], Photovoltaic applications and microwave shielding coatings, Copper Sulphide has also been widely used in many fields as optical filter, solar cell, and ion conduction[10]. Copper Sulphide is often used for ammonia gas sensing at room temperature and these gas sensitive parameters have been found to be dependent upon composition and morphology of Cu_xS materials [11]. Copper Sulfides (Cu_xS, X=1.8-2), are promising candidates as absorbers and/or p-type semiconductors for SSSC (Solid State Solar Cell), because of their structural, optical and electrical properties. The best solar conversion efficiency of almost 6% was reported for the 3D cell using Cu₂S as absorber layer. Cu₂S thin film has been prepared by several deposition techniques such as Solid State Reaction [12], Spray Pyrolysis [13], Sputtering [14] and Vacuum Evaporation [15].

The properties and stoichiometry of the material is often varied due to small difference between the

*Corresponding author

various phases of Cu_xS material and hence it becomes a highly challenging task to deposit Cu_2S film with desired stoichiometric proportion. To the best of our knowledge only a few researchers have reported the annealing effect of Cu_2S film, however a detailed study on the effect of annealing on the properties of these films is still lacking. This paper describes the preparation of Cu_2S films by Vacuum evaporation technique on glass substrate at room temperature and various annealing temperature, and the corresponding change in the structural, optical and resistivity properties of these films with thickness and temperature were carried out in detail.

2. Experimental Details

2.1 Film Deposition

The deposition by thermal method is simple, and most widely used. High purity (99.99%) Copper Sulphide powder was utilized for evaporation. Cleaned optically flat glass substrates were used for preparation. The glass substrates were rinsed with distilled water and placed in an ultrasonic cleaner were agitated for 30 minutes by soap solution and then cleaned with iso-propyl alcohol. Next the glass substrates were heated in a hot air oven in 1 hr at 100°C to remove the volatile impurities. Copper Sulphide powder was placed in molybdenum boat of (200 amps) and heated with high current by energizing transformer. The glass substrate was mounted on a substrate holder with the heating arrangement and the temperature was measured with the help of a fine wire chromel and alumel thermocouple. A constant rate of evaporation $3\text{\AA}/\text{sec}$ was maintained throughout the sample preparation. Rotary drive is employed to maintain uniformity in film thickness. The substrate to source distance was optimized to be at 18.1 cm inside the vacuum chamber. The deposition rate and thickness for all the films were monitored during deposition using quartz crystal monitor and verified by multiple beam interferometer.

2.2. Film Characterization

A simple method used to determine the conductivity type of a specimen is hot probe method. It consists of two fine metal probes placed on the semiconductor sample and galvanometer is connected between them. One probe is maintained at room temperature and the other probe is heated to about 800°C . The hot probe heats the semiconductor beneath it so that the kinetic energy of free carriers in this region is increased. Therefore, the carriers diffuse out of the hot region at a faster rate and the electrons move towards the

hot probe leaving behind the charge carriers of donors. Thus current flows from hot probe to cold probe for all the film studied in this work, and hence it is inferred that Cu_xS film exhibit P-type conductivity.

Structural properties of the film were analysed by a Shimadzu XRD-6000 X-ray diffractometer. Samples were mounted on a specimen holder using silica gel and were scanned at a rate of $0.5^\circ/\text{min}$ with $\text{CuK}\alpha$ radiation. The radiation was filtered using a 1° divergence slit, 1° slatter slit and 0.15 mm receiving slit. All the films were analysed in the $20\text{-}80^\circ(2\theta)$ scale angle range.

The most commonly used technique for measuring resistivity is the four point probe method. This method is non destructive and can be used to measure the resistivity of ingots, as well as wafers. The arrangement consists of PID controlled oven (model-PID-200 scientific equipment and services, Roorkee, India) in combination with low current source (model-LCS-01) and digital micro voltmeter (model-DMV-001). It consists of four collinear metal probes with sharpened tips, which are placed on the flattened surface of the material to be measured. A constant current I is passed through the outer two probes and the potential difference is measured across the inner two probes. The nominal value of the probe spacing is equal to the distance of 2mm between the adjacent probes. The potential difference is measured using a high input impedance voltmeter.

Electrical conductivity of the film with photocurrent was measured by taking silver paste as a contact electrode at 1cm separation applied on the film surface. The samples are kept in the measurement chamber. A halogen lamp was used for white light. The incident light intensity was measured in mW/cm^2 by placing a surya-amp at the position of the sample. The photocurrent was measured using micro ammeter.

3. Results and discussion

3.1. Effect of Film Thickness

It is well known that the various Cu-S phases, namely chalcocite, djurleite, digenite and covellite have different crystallographic structures and hence show different X-ray diffraction patterns. X-ray diffraction can thus be used to identify the Cu-S phases present in vacuum evaporated Cu_2S film. Figures 1, 2, 3 shows the X-ray diffraction patterns of as-deposited Cu_2S thin films of various thicknesses (3000\AA , 5000\AA and 7000\AA) prepared on glass substrates. The crystallinity of the as-deposited films were thought to be amorphous but the presence of humps in Figs. 1 and 2 reveals that the prepared film exhibit a mixed state of the

amorphous and polycrystalline nature of Cu_2S films. However, a strong peak observed in Fig. 3 clearly leads us to understand that the film coated at higher thickness bears polycrystalline nature [16].

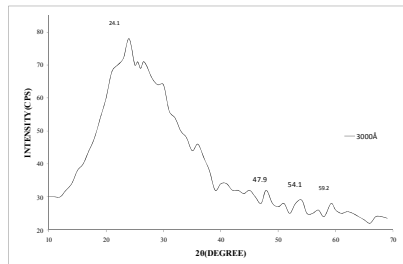


Fig. 1. X-ray diffraction spectra of Cu_2S films of 3000 Å thickness

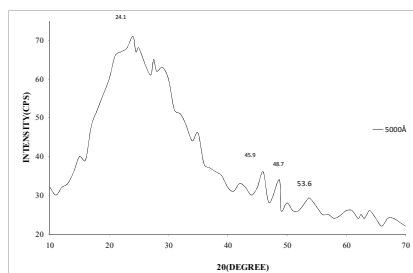


Fig. 2. X-ray diffraction spectra of Cu_2S films of 5000 Å thickness

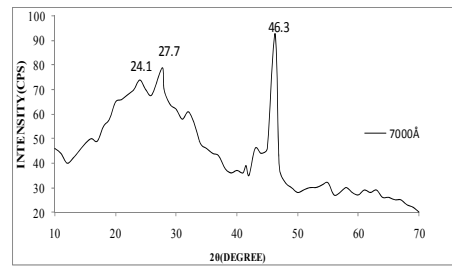


Fig. 3. X-ray diffraction spectra of Cu_2S films of 7000 Å thickness

The peak near $2\theta = 46.78$ in Figs. 1 and 2 is a good diagnostic line for chalcocite Cu_2S phase and is in agreement with the JCPDS value (ISCD 200986). The peaks obtained in XRD spectrum are compared with standard JCPDS values and are reported in Table 1 along with various planes of Cu_2S film. It is thus observed from XRD pattern that the formed film is a mixture of either or both phases of chalcocite (Cu_2S) and covellite (CuS) i. e., Cu_xS with x ($1 < x < 2$). Moreover, (110) plane arrives at 2θ equal to 45.78, 45.91 for films of 3000 Å and 5000 Å thickness respectively.

Table 1. Comparison of observed XRD data of thin films with the JCPDS values

Thickness (Å)	2θ values ($^\circ$)		d-spacing values (Å)		hkl planes	Phase
	Standard	Observed	Standard	Observed		
3000	23.5	24.1	3.72	3.68	002	Cu_2S
	47.4	45.7	1.98	1.98	110	Cu_2S
	52.5	54.1	1.63	1.59	112	CuS
5000	25.9	26.8	3.37	3.60	002	CuS
	47.4	45.9	1.98	1.97	110	Cu_2S
	52.5	54	1.63	1.59	112	Cu_2S
7000	25.9	24.1	3.37	3.43	100	CuS
	27.6	27.7	3.21	3.12	101	CuS
	47.4	46.3	1.90	1.89	110	CuS

In Fig. 3 one small diffraction peak at $2\theta = 27.76$ from (1 0 1) plane and one strong prominent diffraction peak at $2\theta = 46.26$ from (1 1 0) plane are noticed for 7000 Å thickness of Cu_2S films. These peaks near 27.76 and 46.26 are closely associated with covellite phase and no other characteristic phase corresponding to any intermediate Cu_xS structure was obtained. Hence it is noted that, after 5000 Å film thickness the XRD patterns of Cu_2S distinguishes itself from the hexagonal Cu_2S to CuS phases depending on film thickness. Because of sulphur enrichment with minor rearrangements of

copper atoms, the Cu_2S changes its crystal structure from Cu_2S to CuS , i. e., phase transformation exists in the film prepared at higher thickness. Calculated 'd' spacing values are compared with standard JCPDS values of various thicknesses of Cu_2S film and are given in Table 1.

The interplanar distance has been calculated for 3000 Å and 7000 Å film thickness and is reported in Table 2. It is found to be $a = 5.94$ Å, $c = 9.64$ Å for 3000 Å thickness which shows a slight contradiction with the values ($a = 3.95$ Å, $c = 6.78$ Å) reported for Cu_2S Films. The interplanar distance

calculated for 7000 Å film thickness is found to be a =2.99 Å, c= 13.36 Å, which agrees with the values (a=3.79 Å, c=16.34 Å) reported for CuS Films [17]. Deviation in the parameters of these films is connected with lattice mismatch between the atoms in the plane of Cu₂S and the generation of strains within the film [18].

Table 2. Cell parameters value of Cu₂S films of different thicknesses

Thickness (Å)	Cell parameter (Å)		Crystal System	Phase
	Standard	Observed		
3000	a=3.95	a=5.94	Hexagonal	Cu ₂ S
	c=6.78	c=9.64		
7000	a=3.79	a =2.99	Hexagonal	CuS
	c=16.34	c=13.36		

The measured absorbance (A) of the film is related to transmittance (T) by

$$A = \log (1/T) = (I_0/I) \tag{1}$$

where ‘I’ is the transmitted light and ‘I₀’ is the incident light. Figure 4 shows the absorption spectra of Cu₂S thin films measured as a function of wavelength of incident photons for different thicknesses. Absorption spectra of the film decreases at lower thickness and then increases for higher thickness (7000 Å) film. Since it was reported earlier that CuS exhibit metallic conductivity, the higher absorption sample leads us to understand that the sample is a co-vellite phase. Change in the absorption-edge could be examined for various Cu₂S sample and the absorption edge increases with increase in thickness, except at higher thickness sample. Hence the film prepared at higher thickness exhibit lower conduction due to higher absorption behavior of the material.

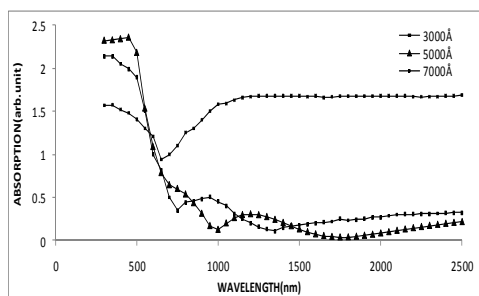


Fig. 4. Absorption spectra of Cu₂S films of different thicknesses

The absorption coefficient (α) is related to band gap (Eg) by

$$\alpha h \nu = (h \nu - E_g)^2 \text{ for indirect transition} \tag{2}$$

where ‘ν’ is the frequency of the incident light and ‘h’ is the Planck’s constant. Band gap of the material can be determined from the plot of

absorption coefficient vs photon energy curve. Extrapolating the straight line portion of the plot of (αhν)² against hν to the energy axis for zero absorption coefficient, the indirect band gap of Cu₂S material is determined for different film thicknesses (Fig. 5) and are reported in Table 3. It is inferred that band gap decreases with increase in film thickness which may be due to change in the barrier height of the crystalline film [19, 20]. The band gap value reported in Table 3 agrees with the earlier values of Cu₂S films.

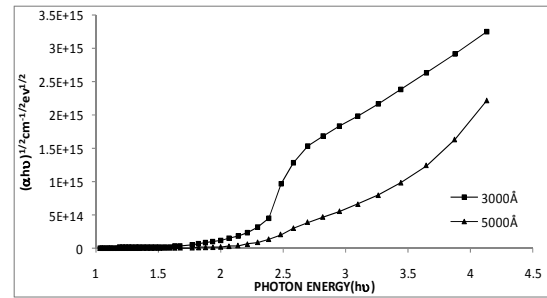


Fig. 5. Variation of absorption coefficient with photon energy for Cu₂S films of different thickness

Table 3. Optical band gap for different film thickness and annealing temperature

Thickness (Å)	Optical Band Gap(e V)	
	Film A	Film C
3000	2.2	2.15
5000	2.1	1.95
7000	1.8	1.72

The most direct method of measuring the sheet resistance is to prepare a rectangular sample of films, divided by the number of squares of the material that lie between the end contacts. The most common form of four point probe is the in-line type. When the materials are placed on the semi-infinite volume, the resistivity is given by

$$\rho = \frac{V}{I} \times 2 \text{ when } S_1=S_2=S_3=S \text{ then}$$

$$\rho = \frac{V}{I} \times 2\pi S = Rs = \frac{\rho}{d} = 4.532 \times \frac{V}{I} \tag{3}$$

where RS is the sheet resistance of the material. A constant current was applied across the sample and the variations of sheet resistance for different thickness was studied in the temperature range (303-453K) and the values are given in Table 4. From Fig. 6 the sheet resistance was found to increase initially and, with further increase in thickness, leads to decrease in resistivity of the film, which may be due to deviation in stoichiometric composition of the films at higher

thickness [21, 22]. Thus the lower thickness film was Cu_2S phase and this decrease in the value of 'x' at higher thickness leads to decrease in sheet resistance of the film. Thus the sample prepared with higher thickness at lower substrate temperature results in phase transformation from chalcocite to co-vellite phase (Cu_2S to CuS). Activation energy for Cu_2S has been calculated from the variation of resistivity with the inverse of temperature curve and the line connecting the $\log \rho$ and $1/T$ gives the slope value. Using the slope value in equation (4), calculated activation energy is given in Table 5.

$$E_g = 2K * \frac{\log \rho}{1/T} \quad (4)$$

Table 4. Sheet resistance for different film thickness and annealing temperature

Thickness (Å)	Sheet resistance (Ω/m)		
	R1 (Film A)	R2 (Film B)	R3 (Film C)
3000	0.35	0.37	0.09
5000	0.382	0.390	0.087
7000	0.020	0.079	0.058

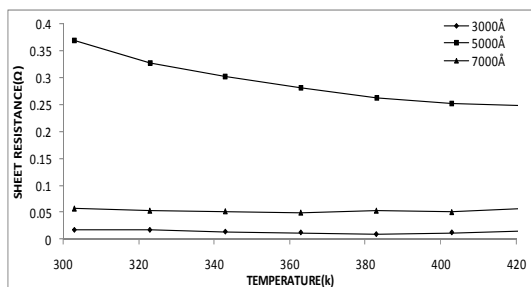


Fig. 6. Variation of sheet resistance with temperature for Cu_2S film of different thickness

Table 5. Activation energy for different film thickness and annealing temperature

Thickness (Å)	Activation energy (eV)		
	E_g (Film A)	E_g (Film B)	E_g (Film C)
3000	0.595	0.395	0.329
5000	0.525	0.329	0.296
7000	0.450	0.197	0.158

The increase in photocurrent with intensity can be described by the relation

$$I_{ph} \propto (In)^m \quad (5)$$

where 'In' is the intensity and 'm' is the integer. Figure 7 shows the light effect on I-V characteristics of Cu_2S film of different thickness for constant illumination. When the film is illuminated by light, additional photo excited carriers are generated in the films; as a result, a part of thermally excited carrier together with large number of photo-generated carriers neutralizes some fraction of localized charges in the depletion

regions in the grain boundary potential barriers. Hence conductivity is found to increase exponentially with applied voltage as well as film thickness [23].

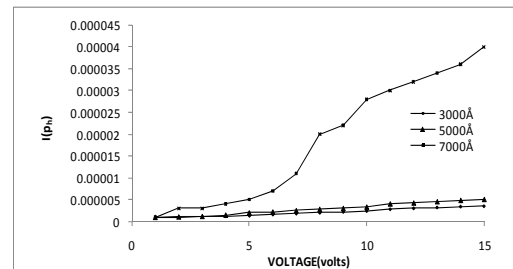


Fig. 7. Variation of Photo-current with voltage for Cu_2S film of different thickness for constant illumination

3.2. Effect of Annealing

The as-deposited film contains voids which influence the resistivity of the film and the defects would anneal out on the application of mild heat treatment. Hence, in order to get it out from the defects the Cu_2S films are annealed at 100°C , 200°C respectively and the properties of the film were examined. As deposited Cu_2S film and the films annealed at 100°C , 200°C are hereafter referred to as Film A, Film B and Film C respectively. Cu_2S sample with the same thickness and coherent are used for the analyses of the film.

3.2.1. At Lower Thickness

Figure 8(a) and (b) represents the SEM image of Cu_2S sample of Film A and Film C for Cu_2S film of 3000 \AA thickness respectively. Figure 8(a) indicates the presence of large size particles of Cu_2S films, where these large size particles disappear when the films are annealed at 200°C 8(b). Moreover, the films tend to condense for higher annealing temperature which indicates a change in the composition of the film as reported by other investigators [24].

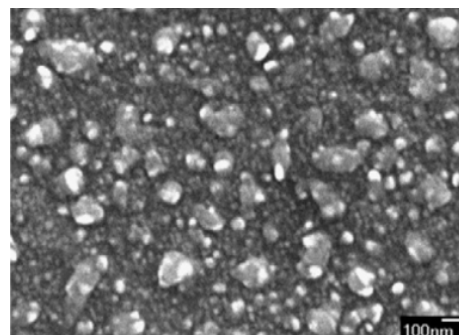


Fig. 8. (a)

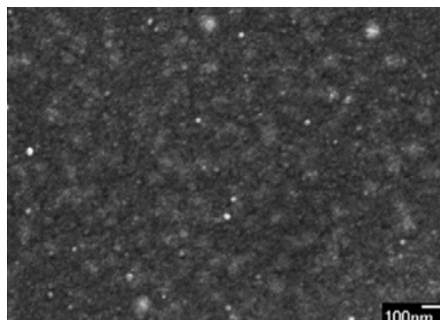


Fig. 8. (a) and (b) SEM image of Film A and Film C of Cu_2S film of 3000 Å thickness

Annealing Cu_2S thin films in air alter the optical properties of the film. The transmittance spectra for different annealing temperature measured as a function of wavelength of incident photons for 3000 Å thickness is shown in Fig. 9. Film B exhibits an increase in transmission, while at the same time a decrease in transmission is noticed for the Film C, which may be due to a change in stoichiometric composition of the film. Therefore it is supposed that the Film C has transformed from Cu_2S to CuS phase [25]. Optical band gap of Cu_2S has been calculated from the plot of absorption coefficient vs Photon energy curve for Film B and Film C of lower thickness sample and the values are given in Table 3. The decrease in band gap energy may be due to the presence of some trace elements in the form of impurities in the film. These impurities can form traps in the forbidden energy gap. It has been reported that the removal of oxygen causes the redistribution of traps and hence a drop in band gap energy.

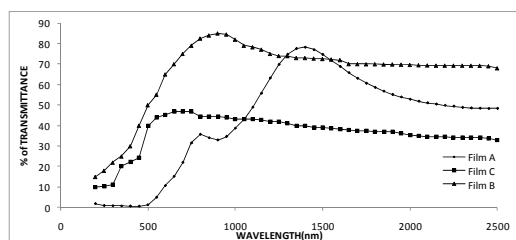


Fig. 9. Variation of transmittance spectra with wavelength for Cu_2S films of 3000 Å thickness at different annealing temperature

Figure 10 shows the variation of sheet resistance as a function of temperature for Cu_2S films of 3000Å thickness at different annealing cycles. The sheet resistance was determined on Film A, Film B and Film C respectively and the values are reported in Table 4. Increase in sheet resistance value is observed for the Film B and further annealing the films at 200°C resulted in significant decrease of sheet resistance with all the Cu_2S films. It is a well-established fact that Cu_2S film exhibit p-type conductivity and this p-type conduction is generally

attributed to free holes from acceptor levels of copper vacancies. The density of this copper vacancy increases as 'x' in Cu_xS decreases from 2 to 1 [26], as a result, there is a decrease in the value of sheet resistance for Film C.

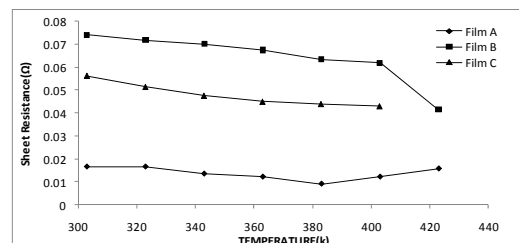


Fig. 10. Variation of sheet resistance with temperature for Cu_2S films of 3000Å thickness at different annealing temperature

The annealing effect on the activation energy of lower thickness Cu_2S sample has been investigated from the variation of resistivity with the inverse of temperature curve and using the slope value in (4). The values given in Table 5 agree with the earlier reports of Cu_2S film [18]. The decrease in activation energy after annealing could be due to the following reasons (i) Presence of the internal electric field with defects present in the film (ii) Improvement in the crystals and increase in the grain size of the film [27].

3.2.2. At Higher Thickness

The transmittance spectra for Cu_2S films of different annealing temperature measured as a function of wavelength for 7000 Å thickness is shown in Fig. 11. All the samples show a peaked transmission in the 600-800nm range but there are differences in transmittance towards higher wavelength. Film A exhibits decrease in transmission in the NIR region as their phase composition is CuS by referring to the previous report of XRD spectrum. Film B and C exhibit increase in transmission, in which Film C exhibits almost similar nature of Film B and maintains the transmittance throughout the rest of the spectrum. Transmission increases with annealing temperature, which is similar to the recent research of Cu_2S film [28]. The result can be explained as, the annealed films mainly consist of Cu_xS phases with increase in x value and these results corroborate that this behavior seems to be associated to the formation of Cu_2S phase [29]. Therefore, it is reported that higher thickness film annealed at higher temperatures have the formation of chalcocite phase (Cu_2S) in common. Optical band gap of Cu_2S has been calculated from the plot of absorption coefficient vs photon energy curve for Film B and Film C of 7000 Å thickness and is reported in Table

3. It is observed that annealing effect does not show significant influence on the band gap of Cu_2S sample and is independent from annealing temperature.

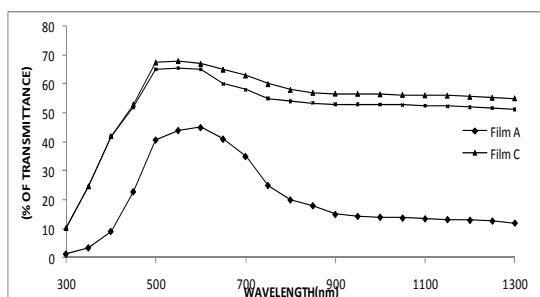


Fig. 11. Variation of transmittance spectra with wavelength for Cu_2S films of 7000 Å thickness at different annealing temperature

The variation of sheet resistance with temperature for 7000Å thickness of Cu_2S sample is shown in Fig. 12 for different annealing temperature. The sheet resistance is found to be linear dependent on temperature for all the cases. It is interesting to note that the sheet resistance increases for the annealed films when compared to Film A. This increase in sheet resistance may be due to greater sulphur deficiency that results in increase in copper content of the film (Table 4). Therefore, when the atomic percent of sulphur decreases, new phases are formed due to the increase in copper content value. It is observed that annealing higher thickness film at higher temperature shows phase transformation from CuS to Cu_2S . Activation energy for 7000Å thickness of Cu_2S film is calculated using (4) for Film B, Film C and the values are reported in Table 5. It is inferred that an increase in annealing temperature causes a decrease in activation energy.

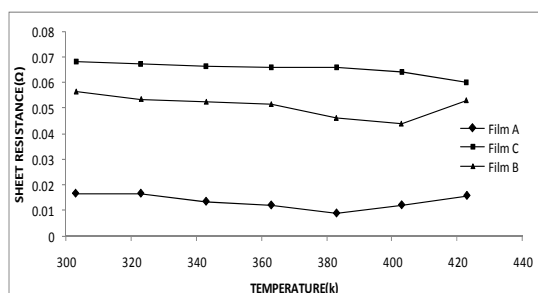


Fig. 12. Variation of sheet resistance with temperature for Cu_2S film of 7000 Å thickness at different annealing temperature

4. Conclusion

Cu_2S thin films of different thicknesses were deposited on glass substrates by vacuum

evaporation method. XRD, Optical and resistivity studies revealed that the film prepared at higher thickness showed a phase transformation. Phase transformation also exist in the film when they are annealed at higher temperature. Hence, in order to obtain high stability chalcocite phase, the samples must be prepared at relatively higher substrate temperature. Moreover, SEM image of the film also confirms the phase transformation from Cu_2S to CuS phase i. e., the material tends to condense during annealing (at 200°C) and this nature is due to the decomposition of films at higher temperature. Thus both temperature and thickness play a vital role in attaining the stoichiometry of Cu_2S film.

References

- [1] Gorai, S., Ganguly, S. & Chaudhuri, S. (2005). Shape selective solvothermal synthesis of copper sulphides: role of ethylenediamine-water solvent system. *Mater. Sci. Eng. B*, 116, 221-225.
- [2] Ramya, M. & Ganesan, S. (2011). Study on current conduction mechanism in evaporated Cu_2S thin films. *Optoelectronics and Advanced Materials-Rapid Communications*, 5, 936-942.
- [3] Lu, Y., Chen, S. L. M. & Jia, J. (2009). Fabrication and characterization of positive and negative copper sulfide micropatterns on self-assembled monolayers. *Journal of Colloid and Interface Science*, 332, 32-38.
- [4] Kuruya, T., Itoh, K. & Sumiyama, K. (2008). Low polydispersed copper-sulfide nanocrystals derived from various Cu-alkyl amine complexes. *Journal of Colloid and interface Science*, 319, 565-571
- [5] Jiang, C., Zhang, W., Zou, G., Xu, L., Yu, W. & Qia, Y. (2005). Hydrothermal fabrication of copper sulfide nanocones and nanobelts. *Materials Letters*, 59, 1008-1011.
- [6] Zhao, S., Han, G. & Li, M. (2010). Fabrication of copper sulfide microstructures with the bottle-and thorny rod-shape. *Materials Chemistry and Physics*, 120, 431-437.
- [7] Xu, N. S. & Huq, S. E. (2005). Novel cold cathode materials and applications. *Mater. Sci. Eng. R*, 48, 47-189.
- [8] Yamamoto, T., Kubota, E., Taniguchi, A., Dev, S., Tanaka, K., Osakada, K. & Sumita, M. (1992). Electrically-conducting metal sulfide-polymer composites prepared by using organosols of metal sulfides. *Chem. Mater.*, 4, 570-576.
- [9] Nair, M. T. S. & Nair, P. K. (1989). Chemical bath deposition of Cu_xS thin films and their prospective large area applications. *Semicond. Sci. Technol.*, 4, 191-199.
- [10] Tang, K., Chen, D., Liu, Y., Shen, G., Zhang, H. & Qian, Y. (2004). Shape-controlled synthesis of copper sulfide nanocrystals via a soft solution route. *Journal of Crystal Growth*, 263, 232-236.
- [11] Gorai, S., Ganguly, D. & Chaudhuri, S. (2007). Morphological control in solvothermal synthesis of copper sulphides on copper foil. *Materials Research Bulletin*, 42, 345-353.

- [12] Burgelman, M. & Vos, A. De. (1983). Evaporation of CuCl and CuCl₂ for the fabrication of Cu₂S/CdS thin film solar cells. *Thin Solid Films*, 102, 367-374.
- [13] Wang, S. Y., Wand, W. & Lu, Z. H. (2003). Asynchronous-pulse ultrasonic spray pyrolysis deposition of Cu_xS (X=1,2) thin films. *Mater. Sci. Eng., B*, 103, 184-188.
- [14] He, Y. B., Polity, A., Österreicher, I., Pfisterer, D., Gregor, R., Meyer, B. K. & Hardt, M. (2001). Hall effect and surface characterization of CuS and CuS films deposited by RF reactive sputtering. *Physica B*, 308-310, 1069-1073.
- [15] Ramya, M. & Ganesan, S. (2012). Role of thickness in physical properties of Cu₂S thin films prepared by vacuum evaporation method. *Journal of Optoelectronics and Advanced Materials*, 14, 910-917.
- [16] Deepa, J., Sathyamoorthy, R. & Subbarayan, A. (2004). Optical properties of thermally evaporated Bi₂Te₃ thin films. *Journal of Crystal Growth*, 274, 100-105.
- [17] Otero, A. L. (1977). The dependence of the grain size of continuous epitaxial films on the growth conditions. *Journal of Crystal Growth*, 42, 157-159.
- [18] Bagul, S. V., Chavhan, S. D. & Sharma, R. (2007). Growth and characterization of Cu_xS (x=1.0, 1.76, and 2.0) thin films grown by solution growth technique (SGT). *Journal of Physics and Chemistry of Solids*, 68, 1623-1629.
- [19] Sathyamoorthy, R., Narayandass, Sa. K. & Mangalraj, D. (2002). Effect of substrate temperature on the structure and optical properties of CdTe thin film. *Solar Energy Materials and Solar Cells*, 76, 339-346.
- [20] Ubale, A. U., Choudhari, D. M., Kantale, K. S., Mitkari, V. S., Nikam, M. S., Gawande, W. J. & Patil, P. P. (2011). Synthesis of nanostructured Cu_xS thin films by chemical route at room temperature and investigation of their size dependent physical properties. *Journal of Alloys and Compounds*, 509, 9249-9254.
- [21] Ducemin, S., Youm, I., Bougnot, J. & Cadene, M. (1987). Fabrication and characterization of sprayed Cd_{1-y}Zn_yS-Cu₂S (dry process) solar cells. *Solar Energy Materials*, 15, 337-350.
- [22] Ramya, M. & Ganesan, S. (2011). Study of thickness dependent characteristics of Cu₂S thin film for various applications. *Iranian Journal of Material Science and Engineering*, 8, 34-40.
- [23] Couve, S., Szepessy, L., Vedel, J. & Castel, E. (1973). Resistivity and optical transmission of Cu_xS layers as a function of composition. *Thin Solid Films*, 15, 223-231.
- [24] Abhay A. Sagade. & Sharma, R. (2008). Copper sulphide (Cu_xS) as an ammonia gas sensor working at room temperature. *Sensors and Actuators B*, 133, 135-143.
- [25] Nien, Y. T. & Chen, I. G. (2009). Rapid thermal annealing of chemical bath-deposited Cu_xS films and their characterization. *Journal of Alloys and Compounds*, 471, 553-556
- [26] Grozdanov, I. & Najdoski, M. (1995). Optical and electrical properties of copper sulfide films of variable composition. *Journal of Solid State Chemistry*, 114, 469-475
- [27] Yildirim, M. A., Ates, A. & Astam, A. (2009). Annealing and light effect on structural, optical and electrical properties of CuS, Cu_{0.6}Zn_{0.4}S and ZnS thin films grown by SILAR method. *Physica E*, 41, 1365-1372.
- [28] Offiah, S. U., Ugwoke, P. E., Ekwealor, A. B. C., Ezugwu, S. C., Osuji, R. U. & Ezema, F. I. (2102). Comparative study of Cu₂S and Cu₂Se thin films grown by CBD. *Digest Journal of Nanomaterials and Biostructures*, 7, 165-173.
- [29] Parrreira, P., Lavareda, G., Amaral, A., Botelho do Rego, A. M., Conde, O., Valente, J., Nunes, F. & Nunes de Carvalho, C. (2011). Transparent p-type Cu_xS thin films. *Journal of Alloys and Compounds*, 509, 5099-5104.